



Published in final edited form as:

Hepatology. 2011 October ; 54(4): 1249–1258. doi:10.1002/hep.24516.

PUMA-mediated apoptosis drives chemical hepatocarcinogenesis in mice

Wei Qiu^{1,#}, Xinwei Wang^{1,#}, Brian Leibowitz¹, Wancai Yang³, Lin Zhang², and Jian Yu^{1,*}

¹Department of Pathology, University of Pittsburgh School of Medicine, University of Pittsburgh Cancer Institute, 5117 Centre Ave., Pittsburgh, PA 15213, USA

²Department of Pharmacology and Chemical Biology, University of Pittsburgh School of Medicine, University of Pittsburgh Cancer Institute, 5117 Centre Ave., Pittsburgh, PA 15213, USA

³University of Illinois at Chicago, Department of Pathology, 840 S. Wood Street, Chicago, IL 60612

Abstract

Hepatocyte death and proliferation contribute to hepatocellular carcinoma development following carcinogen exposure or chronic liver inflammation. However, the role and the molecular targets of hepatocyte death in relation to compensatory proliferation remain to be fully characterized. In this study, we investigated the role of PUMA, a BH3-only protein important for both p53-dependent and -independent apoptosis, in a diethylnitrosamine (DEN)-induced liver carcinogenesis model. PUMA deficiency significantly decreased the multiplicity and size of liver tumors. DEN treatment induced p53-independent PUMA expression, PUMA-dependent hepatocyte death, and compensatory proliferation. Furthermore, inhibition or deletion of JNK1 abrogated PUMA induction, hepatocyte death, and compensatory proliferation. These results provide direct evidence that JNK1/PUMA-dependent apoptosis promotes chemical hepatocarcinogenesis via compensatory proliferation, and suggest apoptotic inducers as potential therapeutic targets in liver injury and cancer.

Keywords

PUMA; JNK1; liver cancer; apoptosis; proliferation

Introduction

Hepatocellular carcinoma (HCC) is the third leading cause of cancer death worldwide (1). Viral hepatitis, alcohol liver disease, and carcinogen exposures are the major risk factors for HCC, and can cause chronic liver injury and inflammation (2). HCC development is commonly associated with hepatocyte death and compensatory proliferation, though the molecular mechanisms underlying hepatocyte death are not well understood (3). Several classes of chemicals promote HCC in rodents (2), including diethylnitrosamine (DEN) that

*Correspondence: Jian Yu, Ph.D., Hillman Cancer Center Research Pavilion, Suite 2.26h, 5117 Centre Ave, Pittsburgh, PA 15213. yuj2@upmc.edu; Phone: 412-623-7786; Fax: 412-623-7778.

#These authors contributed equally to this work.

Author contributions: WQ, WX and BL designed and performed experiments, analyzed data and wrote the paper.

WY performed *JNK1* KO mouse experiment.

LZ provided key reagents.

JY designed experiments, analyzed data and wrote the paper.

Disclosures: The authors have no conflicts to disclose. All authors agreed on the submission.

has been extensively studied and is known to induce rapid killing of hepatocytes (1). A number of signaling pathways have been implicated in DEN-induced liver carcinogenesis. Deficiency of c-jun N-terminal kinase 1 (JNK1) decreased cell death, compensatory proliferation and liver carcinogenesis induced by DEN in mice (4). Inactivation of NF- κ B, a pro-survival factor often over-expressed in cancer, was found to enhance the development of DEN-induced HCC (3). However, lack of positive correlation between apoptosis and susceptibility to DEN-induced hepatocarcinogenesis in mice was reported (5). Therefore, the role and specific mediators of hepatocyte death in HCC development remain to be defined.

The Bcl-2 family of proteins play a central role in apoptosis and cancer development (6). The BH3-only members in this family initiate apoptosis in response to a wide range of stimuli and cell types (7). We and others identified PUMA (p53 up-regulated modulator of apoptosis) as a BH3-only protein that plays an essential role in p53-dependent and -independent apoptosis via the mitochondrial pathway (8–15). Reduced PUMA expression was reported in leukemia and melanoma, while increased PUMA expression led to extensive apoptosis of a variety of human cancer cells *in vitro* and in xenograft models (12, 16, 17). Several lines of evidence demonstrated a prominent role of PUMA in tumor suppression in mice. Inhibition of PUMA by shRNAs suppressed p53-dependent apoptosis, promoted oncogenic transformation of primary murine fibroblasts by E1A/ras, and dramatically accelerated E μ -myc-induced lymphomagenesis (18, 19). Loss of *PUMA* enhanced intestinal tumorigenesis induced by carcinogens or the loss of the APC tumor suppressor (8). Unexpectedly, two independent studies demonstrated that PUMA-dependent apoptosis is required for radiation-induced lymphoma in mice (20, 21), suggesting a complex role of apoptosis in cancer.

Given the strong association of apoptosis and proliferation in HCC development, and the specific death promoting function of PUMA, we investigated the role of PUMA in hepatic carcinogenesis. We found that *PUMA* deficiency significantly decreased DEN-induced liver cancer by blocking the acute apoptotic responses and the subsequent compensatory proliferation. The JNK1/c-Jun pathway, but not p53, appears to be responsible for PUMA induction following DEN treatment. These data provide a novel molecular link between acute tissue injury and cancer development, and offer new avenues for HCC intervention.

Materials and Methods

Mice and Treatment

The procedures for all animal experiments were approved by the Institutional Animal Care and Use Committee at the University of Pittsburgh. The *PUMA* $+/+$ and *PUMA* $-/-$ littermates on C57BL/6 background (F10) were generated from heterozygote intercrosses. The *p53* $-/-$ mice (The Jackson Laboratory) were generated by heterozygote intercrosses. Genotyping was performed as described (9). The *JNK1* $-/-$ mice on C57BL/6 background (F6) were generated by heterozygote intercrosses and were genotyped as previously described (22). The mice were housed in micro isolator cages in a room illuminated from 7:00 AM to 7:00 PM (12:12-hr light-dark cycle), and allowed access to water and chow ad libitum.

For the DEN-induced HCC model (23), DEN (15 mg/kg) was injected intraperitoneally (i.p.) into 15-day-old mice. Mice were sacrificed after 4.5 or 9 months on the standard diet. Surface tumor nodules in each liver lobe were counted and measured with a caliper. For short-term studies of DEN-induced liver injury, eight to twelve week old mice were injected i.p. with DEN (100 mg/kg body weight) and sacrificed after 1, 3, and 10 days. Mice receiving the JNK1 inhibitor, SP600125, were injected with 20 mg/kg i.p. once daily starting 1 day before DEN treatment and continued until 3 days after DEN treatment. All mice were

injected i.p. with 100 mg/kg of bromodeoxyuridine (BrdU) 2 h prior to sacrifice to label cells in S-phase.

ALT Measurement

Venous blood of mice was taken from the tail vein at 0 h, 24 h, and 72 h of DEN treatment. Blood was kept at 4°C for overnight and centrifuged at 200 g for 20 minutes to isolate serum. ALT was measured using the Infinity™ ALT kit (Thermo Scientific, Middletown, VA) and reported as mean ± SD. Briefly, 10 µl serum was added into 100 µl ALT reagent and measured in 37 °C at 340 nm. Each sample was measured in triplicates and three mice were used in each group.

Western Blotting

Total protein was prepared from freshly isolated liver tissue. Approximately 300 mg liver tissue was minced and homogenized in 1 ml homogenization buffer (0.25 M sucrose, 10 mM HEPES, 1 mM EGTA). Extracts were centrifuged at 1000g for 10 minutes, and the supernatant was collected and analyzed by NuPage gel (Invitrogen) electrophoresis as previously described (10). Detailed information on antibodies can be found in the supplemental materials.

Total RNA Extraction and Real-Time Reverse Transcriptase Polymerase Chain Reaction

Approximately 100 mg of fresh tissue was minced and put into 600 µl lysis buffer (Promega). Total RNA was isolated, and cDNA was then generated for real-time PCR analysis as described (9). Real-time PCR was performed on a Mini Opticon Real-time PCR system (Bio-Rad) with SYBR Green (Invitrogen) and primers specific for PUMA and β-actin (10). Melting curve and agarose gel electrophoresis of the PCR products were used to verify the specificity of PCR amplification.

Histological Analysis, TUNEL and BrdU Staining

Liver tissue was fixed in 10% formalin for 24 hr followed by processing. Sections (5µm) from paraffin-embedded liver tissue were subjected to hematoxylin and eosin (H&E) staining for histological analysis and various staining. Protocols for TUNEL and BrdU staining have been described (9, 24). The apoptotic or BrdU index was scored in 900 hepatocytes/mouse and reported as mean SD. Three or more mice were used in each group.

Immunohistochemical (IHC) and Immunofluorescent (IF) staining

Slides were deparaffinized, rehydrated and treated with 3% hydrogen peroxide. Antigen retrieval was performed by boiling the sections for 10 min in 0.1 M Citrate Buffer Antigen Retrieval Solution (pH 6.0). Non-specific antibody binding was blocked using 15% goat serum for 30 min. Detailed information and staining conditions can be found in supplemental materials (24, 25). Cells with positive staining were scored in at least 100 hepatocytes and reported as mean ± SD. Three or more mice were used in each group.

Statistical Analysis

Statistical analysis was carried out using GraphPad Prism V software. Data are presented as mean ± standard deviation. Statistical significance was calculated with a Student's t test. $P < 0.05$ was considered to be significant. The means ± 1 s.d. are shown in the figures where applicable

RESULTS

***PUMA* deficiency attenuated DEN-induced liver cancer**

A single injection of DEN to 15-day-old male mice results in efficient HCC induction (26). To determine a potential role of *PUMA* in chemical hepatocarcinogenesis, we compared the tumor incidence and size in wild-type (WT) and *PUMA*-knockout (*PUMA* KO) littermates 9 months after DEN treatment. All the mice developed tumors by 9 months (Fig. 1A). To our surprise, the tumor incidence in *PUMA* KO mice decreased by about 2-fold compared with WT mice (12.1 ± 5.4 vs. 32.2 ± 7.8) (Fig. 1A and 1B). The overall tumor load was also significantly reduced in *PUMA* KO mice. For example, the relative liver weight versus body weight in *PUMA* KO mice was reduced by 1.5-fold compared to WT mice (2.1 ± 1.1 vs. $5.0 \pm 1.9\%$) (Fig. 1C). The maximal or average size of tumors significantly decreased in *PUMA* KO mice compared to those in WT mice (Fig. 1C and S1A). DEN induces formation of microfoci in the liver of WT mice within 4.5 months of treatment (23), which decreased significantly in *PUMA* KO mice (4.3 ± 2.1 vs. 1.9 ± 1.6) (Fig. 1D and Fig. S1B). These results suggest that *PUMA* is required for efficient HCC induction in response to DEN.

DEN induced *PUMA* expression in the liver

PUMA expression is low or undetectable in unstressed tissues, and is induced by DNA damage or non-genotoxic stimuli by p53-dependent or independent pathways (12). DEN is known to induce DNA damage (27). We therefore analyzed expression of *PUMA* in the liver of WT mice after DEN treatment. Using quantitative RT-PCR, we found that *PUMA* mRNA was induced by 2.5 fold at 24 hours compared to untreated mice (Fig. 2A). *PUMA* protein expression was also significantly elevated at day 3 compared to untreated mice (Fig. 2B). Immunostaining indicated that *PUMA* protein was selectively induced in the hepatocytes around the centrilobular regions 24 hours after DEN treatment, while the basal level was undetectable (IF) (Fig. 2C). A few other BH3-only proteins, such as Bim but not Bad, Noxa, or Bid, were also induced by DEN, while multi BH-domain containing Bcl-2 family members did not show a consistent change (Fig. S2).

***PUMA* deficiency abrogated DEN-induced hepatocyte apoptosis**

DEN induces extensive hepatocyte apoptosis in WT mice within 3 days (Fig. 3A and 3B) (3, 4), notably, in the centrilobular regions where *PUMA* is induced (Figs. 2C and 3B). The apoptosis was suppressed by over 40% in *PUMA* KO mice (Fig. 3A, 3B, and S3). Apoptosis decreased at 10 days in WT mice, but was still higher than that in *PUMA* KO mice (Figs. 3A, 3B and S3). Active caspase-3 staining confirmed these results (Fig. 3C). DEN treatment increased the serum levels of the liver enzyme alanine aminotransferase at day 3 (ALT), which were 40% less in *PUMA* KO mice compared to those in WT mice (Fig. 3D). Since DEN can induce oxidative DNA damage in the liver (3), we evaluated DNA double strand breaks and oxidative DNA damage in the liver with p-H2AX and 8-oHdG staining (28), respectively. No difference in DNA damage was found between WT and *PUMA* KO mice 3 or 10 days after DEN treatment (Fig. S4A–C). Double strand breaks markedly decreased in both WT and *PUMA* KO livers at 10 days (Fig. S4A and S4B).

We then analyzed DNA double strand breaks and apoptosis in HCCs. Very little staining of p-H2AX or apoptosis was found in the tumors, or adjacent normal tissues (Fig. S4E and S4F). The levels of apoptosis and p-H2AX did not differ between WT and *PUMA* KO mice (Fig. S4E, S4F and S5). These results indicate that *PUMA* is a critical mediator of DEN-induced hepatocyte apoptosis and tissue damage, but does not affect basal apoptosis in hepatocytes or established HCCs.

PUMA deficiency attenuated DEN-induced compensatory proliferation

DEN-induced hepatocyte death is associated with compensatory proliferation and HCC development (3, 4). As expected, elevated proliferation was found in the liver of DEN-treated WT mice at 10 days by PCNA and BrdU staining (Figs. 4A, S6A, and S6B). The proliferation centered around the centrilobular regions where apoptotic cells were detected (Fig. S6C). The proliferation was significantly reduced in *PUMA* KO mice compared to WT mice, particularly on day 10 (Figs. 4A and S6). Staining with a mitosis marker phosphorylated-histone 3 (p-H3) also showed reduced mitotic cells in DEN-treated *PUMA* KO mice compared to WT mice (Fig. 4B).

We then analyzed proliferation in the liver tumors in WT and *PUMA* KO mice 9 months after DEN treatment. The numbers of BrdU and PCNA positive cells were reduced by over 70% in *PUMA*-deficient tumors compared to WT tumors (Figs. 4C, 4D, S7A and S7B). However, the proliferation in normal hepatocytes adjacent to the tumors did not show significant difference between WT and *PUMA* KO mice (Fig. S7C and S7D). In addition, the proliferation in the foci was also reduced significantly after 4.5 months DEN treatment in *PUMA* KO mice compared with that in WT mice, but not in the adjacent normal regions (Fig. S8). The numbers and sizes of foci were reduced in *PUMA* KO mice compared to WT mice (Fig. 1D). These results demonstrated that *PUMA* deficiency attenuates DEN-induced compensatory proliferation in hepatocytes and proliferation in HCCs, but has little or no effect on basal proliferation of hepatocytes.

Increased PUMA expression and apoptosis in DEN-induced liver damage is p53-independent

PUMA mediates p53-dependent apoptosis following DNA damage (12, 29). In agreement with other reports, we found that DEN slightly induced p53 protein levels in WT mice (Fig. S2B) (4). To determine whether p53 is required for the induction of PUMA by DEN, we compared PUMA expression and apoptosis in the liver of WT and *p53* KO mice. PUMA was induced by DEN to similar levels in WT and *p53*-deficient mice at day 3 (Fig. 5A). TUNEL and PCNA staining revealed that *p53* deficiency increases, rather than suppresses, DEN-induced hepatocyte death and proliferation (Figs. 5B, 5C and S9). These results indicate that DEN-induced PUMA expression and cell death in hepatocytes is p53 independent.

JNK1/c-Jun pathway is involved in DEN-induced PUMA induction and apoptosis

We further explored the mechanism of PUMA induction by DEN. JNK1 has been implicated in DEN-induced liver injury and HCC (4), and can regulate PUMA expression during fatty acid-induced hepatocyte apoptosis (30). We identified several clustered c-Jun/AP1 binding sites in the mouse and human *PUMA* promoters (Fig. S10). DEN induced JNK activation in the liver of WT mice as indicated by increased phosphorylated-JNK1 (p-JNK1) and phosphorylated c-Jun (p-c-Jun) (Figs. 6A and S2). *PUMA* deficiency did not affect the activation of JNK1 (data not shown).

We then determined a potential role of JNK in DEN-induced PUMA expression, apoptosis and proliferation. The JNK inhibitor SP600125 attenuated DEN-induced PUMA expression in the liver without affecting its basal levels (Figs. 6A, 6B and S11A). SP600125 also blocked DEN-induced hepatocyte apoptosis and compensatory proliferation by over 70% (Figs. 6B and S11CF). Similarly, DEN-induced PUMA expression, hepatocyte apoptosis and compensatory proliferation was suppressed by over 50% in *JNK1* knockout mice (Figs. 6C, 6D and S12). Collectively, these data strongly suggest that the JNK1/PUMA axis contributes critically to DEN-induced hepatocyte apoptosis and subsequent proliferation.

Discussion

Our results indicate that JNK1-dependent PUMA induction mediates DEN-induced hepatocyte apoptosis, proliferation and carcinogenesis. The acute, PUMA-mediated apoptotic response in hepatocytes is a direct cause of compensatory proliferation and ensuing carcinogenesis, underscoring the importance of proliferation as a strong tumor promoter in the liver. Over-expression of Bcl-2 (31) or loss of BH3-only protein Bid suppressed DEN-induced liver cancer and hepatocyte proliferation (23) in mice. Mice deficient in NF- κ B signaling(32) or the antiapoptotic Bcl-2 family member Mcl-1 (33) developed spontaneous HCC secondary to hepatocyte death. These studies strongly argue that apoptosis drives a compensatory proliferation to facilitate carcinogenesis through expansion of mutant cells, consistent with early observations that carcinogens alone resulted in minimal tumor yield in the absence of hepatocyte proliferation (34). Such a conclusion is supported by mathematical modeling (35), in which a high rate of cell death correlated with a great number of cell divisions allows for clonal expansion of cells with more mutations and/or genomic instability. *PUMA* deficiency had little effect on DEN-induced acute DNA damage or repair. It would therefore be interesting to determine whether *PUMA* status modulates chromosomal aberrations in HCC.

A dual role of PUMA and apoptosis in cancer is somewhat surprising but not without precedent. *PUMA* deficiency was recently reported to protect hematopoietic stem/progenitor cells against irradiation-induced cell death, and suppresses compensatory proliferation and lymphomagenesis, which is abrogated by dexamethasone-induced T cell killing (20, 21, 36). Several genes can either promote or suppress tumorigenesis depending on the context. For instance, inactivation of NF- κ B suppressed colitis-induced colon cancer (37), while enhanced the development of DEN-induced HCC (3). Over-expression of Bcl-2 suppressed liver cancer induced by DEN (31), TGF- α (38), c-myc or SV40-T-Ag (39), in contrast to its well-established oncogenic role in other systems (6). The model discussed above (35) might be particularly relevant in understanding carcinogenesis in tissues with high regenerative capacity, such as the liver and hematopoietic system, where strong proliferative responses following acute injuries might favor the selection of cells with deleterious mutations.

Previous studies have established that either p53-dependent or -independent induction of PUMA mediates the apoptotic response to a wide range of stresses (12, 29, 40). JNK1 is important for hepatocyte proliferation under homeostasis (41), and required for DEN-induced HCC (4, 42). Our studies uncover JNK1, but not p53, -dependent, PUMA induction and apoptosis in DEN-induced HCC, perhaps independent of JNK1's ability to regulate cell proliferation (this study) (43). Additional JNK1- or apoptosis-dependent mechanism might contribute to DEN-induced HCC. JNK1 promoted production of cytokines such as TNF- α , IL-6, and HGF (3), and activation of Bim (44). Bim was induced by DEN treatment in the liver (Fig. S2), and regulated Fas-mediated liver damage (45) and hepatitis induced by other agents (44). Mutations in p53, β -catenin, or H-ras have been reported in human or rodent HCCs (46–51), but not found in DEN-induced HCCs in C57BL/6J WT or *PUMA* KO mice (Table S1). Future work is needed to understand and model how cell death and compensatory proliferation can cooperate to initiate and promote the progression of DEN-induced HCC by utilizing specific signaling pathways and its significance in human HCC.

HCC is highly correlated with liver inflammation in human and various experimental animal models (52). DEN or obesity induces TNF- α production to promote liver tumorigenesis (3, 53). Suppression of Myd88-dependent IL-6 production by estrogen explains the resistance of female mice to DEN-induced HCC (54). Mice deficient in NF- κ B signaling were highly susceptible to HCC development, and displayed sustained JNK-activation and production of inflammatory cytokines even in the absence of carcinogen (3, 4, 32). PUMA and apoptosis

was induced by TNF- α or during inflammation through NF- κ B (14, 55). Interestingly, *PUMA*-deficient HCCs or liver foci showed suppressed proliferation long after the initial DEN insult, but little change in apoptosis. Therefore, it is possible that JNK1-mediated production of inflammatory cytokines promotes PUMA-induction, apoptosis and HCC development beyond the initial acute injury phase, providing additional mechanisms between chronic liver injury, inflammation and cancer. This is consistent with higher levels of PUMA in liver tumors compared to adjacent normal tissues in HCC patients (56).

In conclusion, our study has demonstrated that PUMA-mediated apoptosis contributes to carcinogen-induced liver injury, compensatory proliferation and cancer. Inhibition of apoptosis may offer an effective way to protect against hepatic injury and HCC development by reducing the pressure for clonal expansion. Emerging evidence suggests BH3-only proteins as potential therapeutic targets in injury-associated liver disease including cancer (44). Recently developed PUMA inhibitors might be used to test this hypothesis (57).

Supplementary Material

Refer to Web version on PubMed Central for supplementary material.

Acknowledgments

We thank Dr. George Michalopoulos (University of Pittsburgh) for helpful discussion and advice, Hongtao Liu for breeding mice, and Drs. Richard Flavell and Zhinan Yin (Yale University School of Medicine, New Haven, CT) for providing *JNK1*^{-/-} mice.

Funding This work is supported in part by NIH grants CA129829, UO1-DK085570, American Cancer Society grant RGS-10-124-01-CCE and FAMRI (J Yu), and NIH grants CA106348, CA121105, and American Cancer Society grant RSG-07-156-01-CNE (L Zhang).

Abbreviations

PUMA	p53 upregulated modulator of apoptosis
HCC	Hepatocellular carcinoma
DEN	Diethylnitrosamine
TUNEL	terminal deoxynucleotidyl transferase-mediated deoxyuridinetriphosphate nick end labeling
JNK1	C-jun N-terminal kinase 1
PBS	phosphate buffered saline
WT	wild-type
KO	knockout
TNF	tumor necrosis factor
H&E	hematoxylin and eosin

References

1. Thorgeirsson SS, Grisham JW. Molecular pathogenesis of human hepatocellular carcinoma. *Nat Genet.* 2002; 31:339–346. [PubMed: 12149612]
2. Bruix J, Boix L, Sala M, Llovet JM. Focus on hepatocellular carcinoma. *Cancer Cell.* 2004; 5:215–219. [PubMed: 15050913]

3. Maeda S, Kamata H, Luo JL, Leffert H, Karin M. IKKbeta couples hepatocyte death to cytokine-driven compensatory proliferation that promotes chemical hepatocarcinogenesis. *Cell*. 2005; 121:977–990. [PubMed: 15989949]
4. Sakurai T, Maeda S, Chang L, Karin M. Loss of hepatic NF-kappa B activity enhances chemical hepatocarcinogenesis through sustained c-Jun N-terminal kinase 1 activation. *Proc Natl Acad Sci U S A*. 2006; 103:10544–10551. [PubMed: 16807293]
5. Bursch W, Chabicovsky M, Wastl U, Grasl-Kraupp B, Bukowska K, Taper H, Schulte-Hermann R. Apoptosis in stages of mouse hepatocarcinogenesis: failure to counterbalance cell proliferation and to account for strain differences in tumor susceptibility. *Toxicol Sci*. 2005; 85:515–529. [PubMed: 15728704]
6. Adams JM, Cory S. The Bcl-2 apoptotic switch in cancer development and therapy. *Oncogene*. 2007; 26:1324–1337. [PubMed: 17322918]
7. Huang DC, Strasser A. BH3-Only proteins-essential initiators of apoptotic cell death. *Cell*. 2000; 103:839–842. [PubMed: 11136969]
8. Qiu W, Carson-Walter EB, Kuan SF, Zhang L, Yu J. PUMA suppresses intestinal tumorigenesis in mice. *Cancer Res*. 2009; 69:4999–5006. [PubMed: 19491259]
9. Qiu W, Carson-Walter EB, Liu H, Epperly M, Greenberger JS, Zambetti GP, Zhang L, et al. PUMA regulates intestinal progenitor cell radiosensitivity and gastrointestinal syndrome. *Cell Stem Cell*. 2008; 2:576–583. [PubMed: 18522850]
10. Qiu W, Leibowitz B, Zhang L, Yu J. Growth factors protect intestinal stem cells from radiation-induced apoptosis by suppressing PUMA through the PI3K/AKT/p53 axis. *Oncogene*. 2010; 29:1622–1632. [PubMed: 19966853]
11. Wu B, Qiu W, Wang P, Yu H, Cheng T, Zambetti GP, Zhang L, et al. p53 independent induction of PUMA mediates intestinal apoptosis in response to ischaemia-reperfusion. *Gut*. 2007; 56:645–654. [PubMed: 17127703]
12. Yu J, Zhang L. PUMA, a potent killer with or without p53. *Oncogene*. 2008; 27(Suppl 1):S71–83. [PubMed: 19641508]
13. Hwang PM, Bunz F, Yu J, Rago C, Chan TA, Murphy MP, Kelso GF, et al. Ferredoxin reductase affects p53-dependent, 5-fluorouracil-induced apoptosis in colorectal cancer cells. *Nat Med*. 2001; 7:1111–1117. [PubMed: 11590433]
14. Wang P, Qiu W, Dudgeon C, Liu H, Huang C, Zambetti GP, Yu J, et al. PUMA is directly activated by NF-kappaB and contributes to TNF-alpha-induced apoptosis. *Cell Death Differ*. 2009; 16:1192–1202. [PubMed: 19444283]
15. Villunger A, Michalak EM, Coultas L, Mullauer F, Bock G, Ausserlechner MJ, Adams JM, et al. p53- and Drug-Induced Apoptotic Responses Mediated by BH3-Only Proteins Puma and Noxa. *Science*. 2003; 302:1036–1038. [PubMed: 14500851]
16. Yu J, Yue W, Wu B, Zhang L. PUMA sensitizes lung cancer cells to chemotherapeutic agents and irradiation. *Clin Cancer Res*. 2006; 12:2928–2936. [PubMed: 16675590]
17. Sun Q, Sakaida T, Yue W, Gollin SM, Yu J. Chemosensitization of head and neck cancer cells by PUMA. *Mol Cancer Ther*. 2007; 6:3180–3188. [PubMed: 18089712]
18. Hemann MT, Zilfou JT, Zhao Z, Burgess DJ, Hannon GJ, Lowe SW. Suppression of tumorigenesis by the p53 target PUMA. *Proc Natl Acad Sci U S A*. 2004; 101:9333–9338. [PubMed: 15192153]
19. Garrison SP, Jeffers JR, Yang C, Nilsson JA, Hall MA, Rehg JE, Yue W, et al. Selection against PUMA gene expression in Myc-driven B-cell lymphomagenesis. *Mol Cell Biol*. 2008; 28:5391–5402. [PubMed: 18573879]
20. Labi V, Erlacher M, Krumschnabel G, Manzl C, Tzankov A, Pinon J, Egle A, et al. Apoptosis of leukocytes triggered by acute DNA damage promotes lymphoma formation. *Genes Dev*. 2010; 24:1602–1607. [PubMed: 20679395]
21. Michalak EM, Vandenberg CJ, Delbridge AR, Wu L, Scott CL, Adams JM, Strasser A. Apoptosis-promoted tumorigenesis: gamma-irradiation-induced thymic lymphomagenesis requires Puma-driven leukocyte death. *Genes Dev*. 2010; 24:1608–1613. [PubMed: 20679396]
22. Tong C, Yin Z, Song Z, Dockendorff A, Huang C, Mariadason J, Flavell RA, et al. c-Jun NH2-terminal kinase 1 plays a critical role in intestinal homeostasis and tumor suppression. *Am J Pathol*. 2007; 171:297–303. [PubMed: 17591974]

23. Bai L, Ni HM, Chen X, DiFrancesca D, Yin XM. Deletion of Bid impedes cell proliferation and hepatic carcinogenesis. *Am J Pathol.* 2005; 166:1523–1532. [PubMed: 15855651]
24. Leibowitz BJ, Qiu W, Liu H, Cheng T, Zhang L, Yu J. Uncoupling p53 Functions in Radiation-Induced Intestinal Damage via PUMA and p21. *Mol Cancer Res.* 2011; 9:616–625. [PubMed: 21450905]
25. Qiu W, Wang X, Leibowitz B, Liu H, Barker N, Okada H, Oue N, et al. Chemoprevention by nonsteroidal anti-inflammatory drugs eliminates oncogenic intestinal stem cells via SMAC-dependent apoptosis. *Proc Natl Acad Sci U S A.* 2010; 107:20027–20032. [PubMed: 21041628]
26. Vesselinovitch SD, Koka M, Mihailovich N, Rao KV. Carcinogenicity of diethylnitrosamine in newborn, infant, and adult mice. *J Cancer Res Clin Oncol.* 1984; 108:60–65. [PubMed: 6746718]
27. Feinberg A, Zedeck MS. Production of a highly reactive alkylating agent from the organospecific carcinogen methylazoxymethanol by alcohol dehydrogenase. *Cancer Res.* 1980; 40:4446–4450. [PubMed: 7002292]
28. Kasai H. Analysis of a form of oxidative DNA damage, 8-hydroxy-2'-deoxyguanosine, as a marker of cellular oxidative stress during carcinogenesis. *Mutat Res.* 1997; 387:147–163. [PubMed: 9439711]
29. Sun Q, Ming L, Thomas SM, Wang Y, Chen ZG, Ferris RL, Grandis JR, et al. PUMA mediates EGFR tyrosine kinase inhibitor-induced apoptosis in head and neck cancer cells. *Oncogene.* 2009; 18:2348–2357. [PubMed: 19421143]
30. Cazanave SC, Mott JL, Elmi NA, Bronk SF, Werneburg NW, Akazawa Y, Kahraman A, et al. JNK1-dependent PUMA expression contributes to hepatocyte lipoapoptosis. *J Biol Chem.* 2009; 284:26591–26602. [PubMed: 19638343]
31. Pierce RH, Vail ME, Ralph L, Campbell JS, Fausto N. Bcl-2 expression inhibits liver carcinogenesis and delays the development of proliferating foci. *Am J Pathol.* 2002; 160:1555–1560. [PubMed: 12000706]
32. Luedde T, Beraza N, Kotsikoris V, van Loo G, Nenci A, De Vos R, Roskams T, et al. Deletion of NEMO/IKKgamma in liver parenchymal cells causes steatohepatitis and hepatocellular carcinoma. *Cancer Cell.* 2007; 11:119–132. [PubMed: 17292824]
33. Weber A, Boger R, Vick B, Urbanik T, Haybaeck J, Zoller S, Teufel A, et al. Hepatocyte-specific deletion of the antiapoptotic protein myeloid cell leukemia-1 triggers proliferation and hepatocarcinogenesis in mice. *Hepatology.* 2010; 51:1226–1236. [PubMed: 20099303]
34. Peraino C, Staffeldt EF, Carnes BA, Ludeman VA, Blomquist JA, Vesselinovitch SD. Characterization of histochemically detectable altered hepatocyte foci and their relationship to hepatic tumorigenesis in rats treated once with diethylnitrosamine or benzo(a)pyrene within one day after birth. *Cancer Res.* 1984; 44:3340–3347. [PubMed: 6331643]
35. Wodarz D, Komarova N. Can loss of apoptosis protect against cancer? *Trends Genet.* 2007; 23:232–237. [PubMed: 17382429]
36. Yu H, Shen H, Yuan Y, XuFeng R, Hu X, Garrison SP, Zhang L, et al. Deletion of Puma protects hematopoietic stem cells and confers long-term survival in response to high-dose gamma-irradiation. *Blood.* 2010; 115:3472–3480. [PubMed: 20177048]
37. Greten FR, Eckmann L, Greten TF, Park JM, Li ZW, Egan LJ, Kagnoff MF, et al. IKKbeta links inflammation and tumorigenesis in a mouse model of colitis-associated cancer. *Cell.* 2004; 118:285–296. [PubMed: 15294155]
38. Vail ME, Pierce RH, Fausto N. Bcl-2 delays and alters hepatic carcinogenesis induced by transforming growth factor alpha. *Cancer Res.* 2001; 61:594–601. [PubMed: 11212255]
39. de La Coste A, Mignon A, Fabre M, Gilbert E, Porteu A, Van Dyke T, Kahn A, et al. Paradoxical inhibition of c-myc-induced carcinogenesis by Bcl-2 in transgenic mice. *Cancer Res.* 1999; 59:5017–5022. [PubMed: 10519417]
40. Ming L, Sakaida T, Yue W, Jha A, Zhang L, Yu J. Sp1 and p73 Activate PUMA Following Serum Starvation. *Carcinogenesis.* 2008; 29:1878–1884. [PubMed: 18579560]
41. Sabapathy K, Hochedlinger K, Nam SY, Bauer A, Karin M, Wagner EF. Distinct roles for JNK1 and JNK2 in regulating JNK activity and c-Jun-dependent cell proliferation. *Mol Cell.* 2004; 15:713–725. [PubMed: 15350216]

42. Eferl R, Ricci R, Kenner L, Zenz R, David JP, Rath M, Wagner EF. Liver tumor development. c-Jun antagonizes the proapoptotic activity of p53. *Cell*. 2003; 112:181–192. [PubMed: 12553907]
43. Finnberg N, Stenius U, Hogberg J. Heterozygous p53-deficient (+/-) mice develop fewer p53-negative preneoplastic focal liver lesions in response to treatment with diethylnitrosamine than do wild-type (+/+) mice. *Cancer Lett*. 2004; 207:149–155. [PubMed: 15072823]
44. Kaufmann T, Jost PJ, Pellegrini M, Puthalakath H, Gugasyan R, Gerondakis S, Cretney E, et al. Fatal hepatitis mediated by tumor necrosis factor TNFalpha requires caspase-8 and involves the BH3-only proteins Bid and Bim. *Immunity*. 2009; 30:56–66. [PubMed: 19119023]
45. Corazza N, Jakob S, Schaer C, Frese S, Keogh A, Stroka D, Kassahn D, et al. TRAIL receptor-mediated JNK activation and Bim phosphorylation critically regulate Fas-mediated liver damage and lethality. *J Clin Invest*. 2006; 116:2493–2499. [PubMed: 16955144]
46. Farazi PA, DePinho RA. Hepatocellular carcinoma pathogenesis: from genes to environment. *Nat Rev Cancer*. 2006; 6:674–687. [PubMed: 16929323]
47. Kress S, Konig J, Schweizer J, Lohrke H, Bauer-Hofmann R, Schwarz M. p53 mutations are absent from carcinogen-induced mouse liver tumors but occur in cell lines established from these tumors. *Mol Carcinog*. 1992; 6:148–158. [PubMed: 1382443]
48. Schwarz M, Wanke I, Wulbrand U, Moennikes O, Buchmann A. Role of connexin32 and beta-catenin in tumor promotion in mouse liver. *Toxicol Pathol*. 2003; 31:99–102. [PubMed: 12597453]
49. Buchmann A, Bauer-Hofmann R, Mahr J, Drinkwater NR, Luz A, Schwarz M. Mutational activation of the c-Ha-ras gene in liver tumors of different rodent strains: correlation with susceptibility to hepatocarcinogenesis. *Proc Natl Acad Sci U S A*. 1991; 88:911–915. [PubMed: 1992483]
50. Hussain SP, Schwank J, Staib F, Wang XW, Harris CC. TP53 mutations and hepatocellular carcinoma: insights into the etiology and pathogenesis of liver cancer. *Oncogene*. 2007; 26:2166–2176. [PubMed: 17401425]
51. Kim CM, Koike K, Saito I, Miyamura T, Jay G. HBx gene of hepatitis B virus induces liver cancer in transgenic mice. *Nature*. 1991; 351:317–320. [PubMed: 2034275]
52. He G, Karin M. NF-kappaB and STAT3 - key players in liver inflammation and cancer. *Cell Res*. 2011; 21:159–168. [PubMed: 21187858]
53. Park EJ, Lee JH, Yu GY, He G, Ali SR, Holzer RG, Osterreicher CH, et al. Dietary and genetic obesity promote liver inflammation and tumorigenesis by enhancing IL-6 and TNF expression. *Cell*. 2010; 140:197–208. [PubMed: 20141834]
54. Naugler WE, Sakurai T, Kim S, Maeda S, Kim K, Elsharkawy AM, Karin M. Gender disparity in liver cancer due to sex differences in MyD88-dependent IL-6 production. *Science*. 2007; 317:121–124. [PubMed: 17615358]
55. Qiu W, Wu B, Wang X, Buchanan ME, Regueiro MD, Hartman DJ, Schoen RE, et al. PUMA-mediated intestinal epithelial apoptosis contributes to ulcerative colitis in humans and mice. *J Clin Invest*. 2011; 121:1722–1732. [PubMed: 21490394]
56. Ahn CH, Jeong EG, Kim SS, Lee JW, Lee SH, Kim SH, Kim MS, et al. Expressional and mutational analysis of pro-apoptotic Bcl-2 member PUMA in hepatocellular carcinomas. *Dig Dis Sci*. 2008; 53:1395–1399. [PubMed: 17934815]
57. Mustata G, Li M, Zevola N, Bakan A, Zhang L, Epperly M, Greenberger JS, et al. Development of small-molecule PUMA inhibitors for mitigating radiation-induced cell death. *Curr Top Med Chem*. 2011; 11:281–290. [PubMed: 21320058]

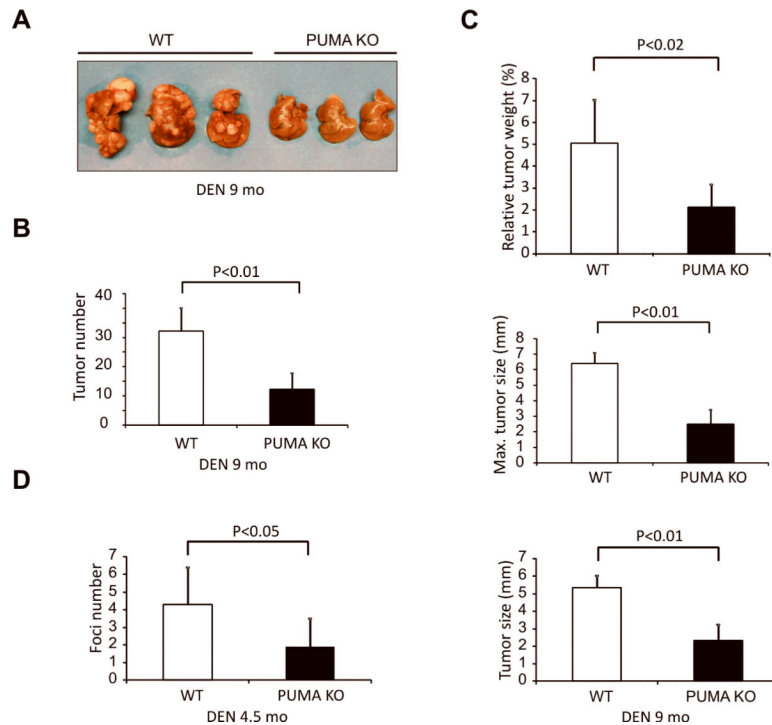


Figure 1. *PUMA* deficiency suppressed DEN-induced liver cancer

WT and *PUMA* KO mice were treated with a single 100 mg/kg injection of DEN and livers were harvested at 9 or 4.5 months. (A) Representative pictures of DEN-induced liver tumors at 9 months. (B) Quantification of liver tumors in WT and *PUMA* KO mice at 9 months. Values are means \pm SD, $n = 8$ mice in each group. (C) *Top*, quantification of average liver weight as a percentage of body weight. *Middle*, quantification of maximal tumor size (diameter) by caliper. *Bottom*, quantification of average liver tumor size (diameter) by caliper. Values are means \pm SD, $n = 8$ mice in each group, 9 months after DEN administration. (D) Quantification of liver microfoci at 4.5 months. Values are means \pm SD, $n = 6$ mice in each group.

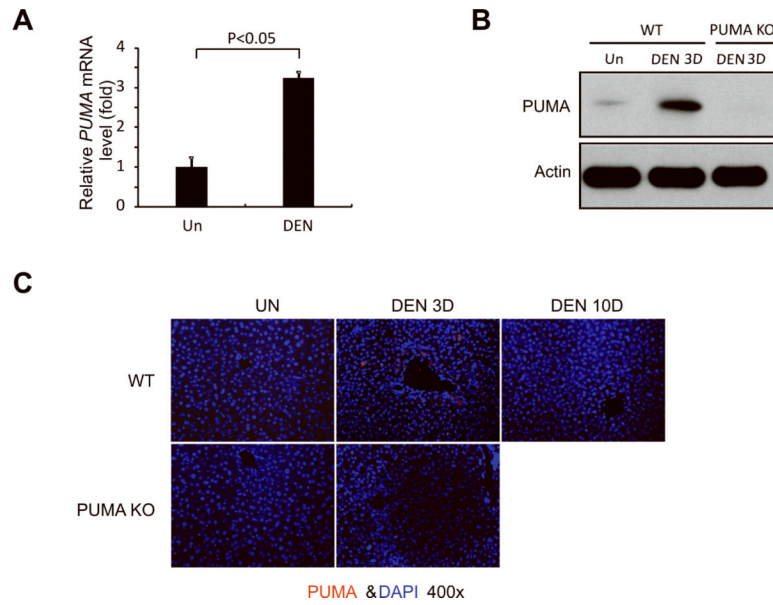


Figure 2. DEN treatment induced PUMA expression in the liver

(A) *PUMA* mRNA expression in the liver of WT mice 3 days following injection with either saline (Un) or 100 mg/kg of DEN was analyzed by quantitative RT-PCR. Values are means \pm SD, $n = 3$ mice in each group. (B) *PUMA* protein expression in the liver of WT and *PUMA* KO mice was determined by Western blotting 3 days after AOM injection. β -actin was used as the control for loading ($n = 3$ mice in each group). (C) *PUMA* protein (red) in the liver of WT and *PUMA* KO mice following indicated treatment was detected by IF with nuclei counterstained with DAPI (magnification, $\times 400$).

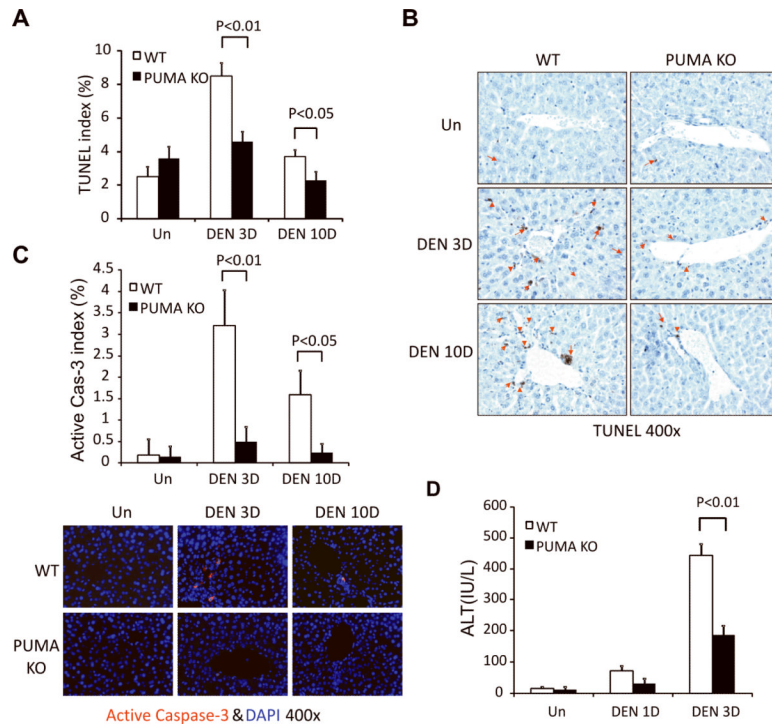


Figure 3. PUMA mediated DEN-induced apoptosis in the liver

Liver tissue or blood was harvested from WT and *PUMA* KO mice 0, 1, 3, or 10 days after a single 100 mg/kg injection of DEN. **(A)** Index of TUNEL positive cells in the liver was measured by counting 900 cells/mouse. Values are means \pm SD, $n = 3$ mice in each group. **(B)** Examples of TUNEL IHC staining (brown) in the liver are indicated by red arrows (magnification, $\times 400$). **(C)** Index of active caspase 3 positive cells in the liver was measured by counting 900 cells/mouse (magnification, $\times 400$). Values are means \pm SD, $n = 3$ mice in each group. *Lower*, examples of active caspase 3 IF staining (red) in the liver with nuclei counterstained with DAPI (magnification, $\times 400$). **(D)** Serum alanine aminotransferase (ALT) levels were determined at the indicated time points after DEN treatment. Values are means \pm SD, $n = 3$ mice in each group.

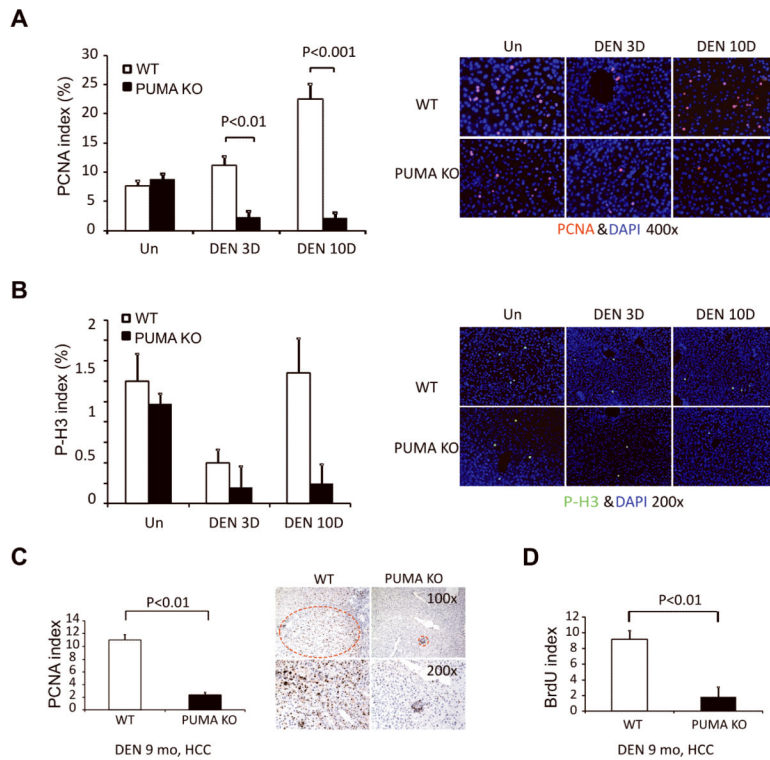


Figure 4. PUMA deficiency suppressed DEN-induced compensatory proliferation in hepatocytes and tumor proliferation

(A) Liver tissue was harvested from WT and *PUMA* KO mice 0, 3, and 10 days after injection of 100 mg/kg of DEN. PCNA index at indicated time points was quantitated by counting 900 cells/mouse. Values are means \pm SD, $n = 3$ mice in each group. *Right*, representative pictures of PCNA staining (red) with nuclei counterstained with DAPI (magnification, $\times 400$). (B) p-H3 staining index in the liver at indicated times after DEN treatment was quantitated by counting 900 cells/mouse. Values are means \pm SD, $n = 3$ mice in each group. *Right*, representative pictures of p-H3 staining (green) with nuclei counterstained with DAPI (magnification, $\times 200$). (C) PCNA index in DEN-induced liver tumors 9 months after treatment was quantitated by counting 900 cells/mouse. Values are means \pm SD, $n = 3$ mice in each group. Representative pictures are shown on the right with tumors circled (magnification, $\times 100$ and $\times 200$). (D) BrdU incorporation index in DEN-induced liver tumors 9 months after treatment was quantitated by counting 900 cells/mouse. Values are means \pm SD, $n = 3$ mice in each group.

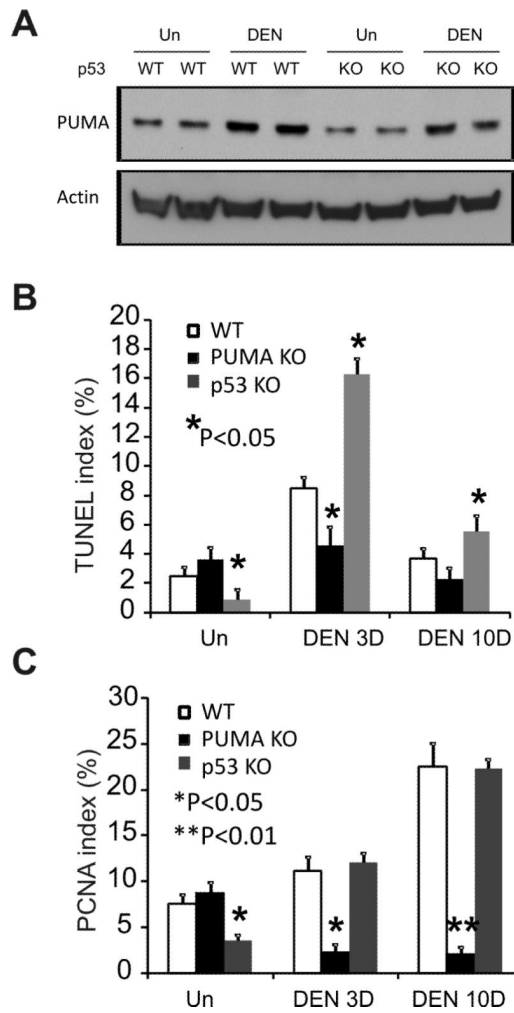


Figure 5. PUMA-mediated apoptosis induced by DEN in the liver is p53-independent
 Liver tissue was harvested from WT, *PUMA* KO or *p53* KO mice 0, 3, and 10 days after 100 mg/kg of DEN injection. (A) The expression of PUMA in the liver was analyzed by Western blotting 3 days after DEN treatment. Actin was used as the control for loading. (B) TUNEL index was calculated by counting 900 cells/mouse at the indicated time points after DEN treatment. Values are means \pm SD, $n = 3$ mice in each group. *P, vs. WT for the same treatment. (C) PCNA index in the liver at the indicated time points after DEN treatment was quantitated by counting 900 cells/mouse. Values are means \pm SD, $n = 3$ mice in each group. *P, **P, vs. WT for the same treatment.

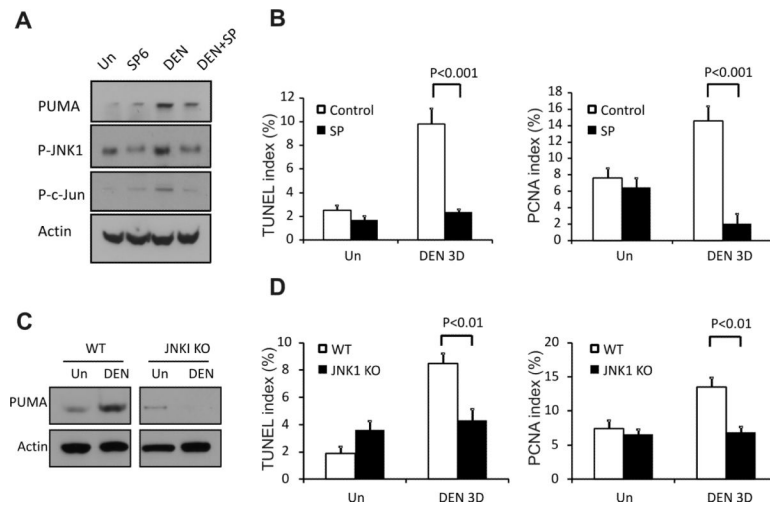


Figure 6. Inhibition of JNK1 abrogated DEN-induced PUMA induction, cell death, and compensatory proliferation

(A) WT mice were injected i.p. with SP600125 daily for 4 days, starting 1 day before DEN treatment and continued until 3 days after DEN treatment. The expression of PUMA, p-JNK, and p-c-Jun in the liver with the indicated treatment was determined by Western blotting. Actin was used as the control for loading. (B) The TUNEL and PCNA indices were calculated following respective staining by counting 900 cells/mouse at 3 days with the indicated treatment. Values are means \pm SD, $n = 3$ mice in each group. (C) Liver tissue was harvested 0 and 3 days after 100 mg/kg DEN injection from WT or *JNK1* KO mice. The expression of PUMA in the liver was determined by Western blotting. Actin was used as a control for loading. (D) TUNEL and PCNA indices were calculated following respective staining by counting 900 cells/mouse with indicated treatment on day 0 or 3 of DEN treatment in WT and *JNK1* KO mice. Values are means \pm SD, $n = 3$ mice in each group.